The Astrophysical Journal, 861:85 (10pp), 2018 July 10 https://doi.org/10.3847/1538-4357/aac515

Fermi-LAT Observations of LIGO/Virgo Event GW170817

M. Ajello[1], A. Allafort[2], M. Axelsson[3,4], L. Baldini[5], G. Barbiellini[6,7], M. G. Baring[8], D. Bastieri[9,10], R. Bellazzini[11], B. Berenji[12], E. Bissaldi[13,14], R. D. Blandford[2], E. D. Bloom[2], R. Bonino[15,16], E. Bottacini[2], T. J. Brandt[17], J. Bregeon[18], P. Bruel[19], R. Buehler[20], T. H. Burnett[21], S. Buson[17,67], R. A. Cameron[2], R. Caputo[22], P. A. Caraveo[23], J. M. Casandjian[24], E. Cavazzuti[25], A. Chekhtman[26], C. C. Cheung[27], J. Chiang[2], G. Chiaro[23], S. Ciprini[28,29], J. Cohen-Tanugi[18], L. R. Cominsky[30], D. Costantin[10], A. Cuoco[15,31], S. Cutini[28,29], F. D'Ammando[32,33], F. de Palma[14,34], N. Di Lalla[5], M. Di Mauro[2], L. Di Venere[13,14], R. Dubois[2], D. Dumora[35], C. Favuzzi[13,14], E. C. Ferrara[17], A. Franckowiak[20], Y. Fukazawa[36], S. Funk[37], P. Fusco[13,14], F. Gargano[14], D. Gasparrini[28,29], N. Giglietto[13,14], R. Gill[38], F. Giordano[13,14], M. Giroletti[32], T. Glanzman[2], J. Granot[38], D. Green[17,39], I. A. Grenier[24], M.-H. Grondin[35], L. Guillemot[40,41], S. Guiriec[17,42], A. K. Harding[17], E. Hays[17], D. Horan[19], F. Imazato[36], G. Jóhannesson[43,44], T. Kamae[45], S. Kensei[36], D. Kocevski[17], M. Kuss[11], G. La Mura[10], S. Larsson[3,46], L. Latronico[15], J. Li[47], F. Longo[6,7], F. Loparco[13,14], M. N. Lovellette[27], P. Lubrano[29], J. D. Magill[39], S. Maldera[15], A. Manfreda[5], M. N. Mazziotta[14], P. F. Michelson[2], T. Mizuno[48], A. A. Moiseev[22,39], M. E. Monzani[2], E. Moretti[49], A. Morselli[50], I. V. Moskalenko[2], M. Negro[15,16], E. Nuss[18], R. Ojha[17], N. Omodei[2], E. Orlando[2], J. F. Ormes[51], M. Palatiello[6,7], V. S. Paliya[1], D. Paneque[49], M. Persic[6,52], M. Pesce-Rollins[11], V. Petrosian[2], F. Piron[18], T. A. Porter[2], G. Principe[37], J. L. Racusin[17], S. Rainò[13,14], R. Rando[9,10], M. Razzano[11,68], S. Razzaque[53], A. Reimer[2,54], O. Reimer[2,54], S. Ritz[55], L. S. Rochester[2], F. Ryde[3,46], P. M. Saz Parkinson[55,56,57], C. Sgrò[11], E. J. Siskind[58], F. Spada[11], G. Spandre[11], P. Spinelli[13,14], D. J. Suson[59], H. Tajima[2,60], M. Takahashi[49], D. Tak[17,39], J. G. Thayer[2], J. B. Thayer[2], D. F. Torres[47,61], E. Torresi[62], G. Tosti[29,63], E. Troja[17,39], J. Valverde[19], T. M. Venters[17], G. Vianello[2], K. Wood[64], C. Yang[36], and G. Zaharijas[65,66]

[1] Department of Physics and Astronomy, Clemson University, Kinard Lab of Physics, Clemson, SC 29634-0978, USA
[2] W.W. Hansen Experimental Physics Laboratory, Kavli Institute for Particle Astrophysics and Cosmology, Department of Physics and SLAC National Accelerator Laboratory, Stanford University, Stanford, CA 94305, USA; nicola.omodei@stanford.edu, giacomov@slac.stanford.edu
[3] Department of Physics, KTH Royal Institute of Technology, AlbaNova, SE-106 91 Stockholm, Sweden
[4] Tokyo Metropolitan University, Department of Physics, Minami-osawa 1-1, Hachioji, Tokyo 192-0397, Japan
[5] Università di Pisa and Istituto Nazionale di Fisica Nucleare, Sezione di Pisa I-56127 Pisa, Italy
[6] Istituto Nazionale di Fisica Nucleare, Sezione di Trieste, I-34127 Trieste, Italy
[7] Dipartimento di Fisica, Università di Trieste, I-34127 Trieste, Italy
[8] Rice University, Department of Physics and Astronomy, MS-108, P.O. Box 1892, Houston, TX 77251, USA
[9] Istituto Nazionale di Fisica Nucleare, Sezione di Padova, I-35131 Padova, Italy
[10] Dipartimento di Fisica e Astronomia "G. Galilei," Università di Padova, I-35131 Padova, Italy
[11] Istituto Nazionale di Fisica Nucleare, Sezione di Pisa, I-56127 Pisa, Italy
[12] California State University, Los Angeles, Department of Physics and Astronomy, Los Angeles, CA 90032, USA
[13] Dipartimento di Fisica "M. Merlin" dell'Università e del Politecnico di Bari, I-70126 Bari, Italy
[14] Istituto Nazionale di Fisica Nucleare, Sezione di Bari, I-70126 Bari, Italy
[15] Istituto Nazionale di Fisica Nucleare, Sezione di Torino, I-10125 Torino, Italy
[16] Dipartimento di Fisica, Università degli Studi di Torino, I-10125 Torino, Italy
[17] NASA Goddard Space Flight Center, Greenbelt, MD 20771, USA; kocevski@slac.stanford.edu
[18] Laboratoire Univers et Particules de Montpellier, Université Montpellier, CNRS/IN2P3, F-34095 Montpellier, France
[19] Laboratoire Leprince-Ringuet, École polytechnique, CNRS/IN2P3, F-91128 Palaiseau, France
[20] Deutsches Elektronen Synchrotron DESY, D-15738 Zeuthen, Germany
[21] Department of Physics, University of Washington, Seattle, WA 98195-1560, USA
[22] Center for Research and Exploration in Space Science and Technology (CRESST) and NASA Goddard Space Flight Center, Greenbelt, MD 20771, USA
[23] INAF-Istituto di Astrofisica Spaziale e Fisica Cosmica Milano, via E. Bassini 15, I-20133 Milano, Italy
[24] Laboratoire AIM, CEA-IRFU/CNRS/Université Paris Diderot, Service d'Astrophysique, CEA Saclay, F-91191 Gif sur Yvette, France
[25] Italian Space Agency, Via del Politecnico snc, I-00133 Roma, Italy
[26] College of Science, George Mason University, Fairfax, VA 22030, resident at Naval Research Laboratory, Washington, DC 20375, USA
[27] Space Science Division, Naval Research Laboratory, Washington, DC 20375-5352, USA
[28] Space Science Data Center—Agenzia Spaziale Italiana, Via del Politecnico, snc, I-00133 Roma, Italy
[29] Istituto Nazionale di Fisica Nucleare, Sezione di Perugia, I-06123 Perugia, Italy
[30] Department of Physics and Astronomy, Sonoma State University, Rohnert Park, CA 94928-3609, USA
[31] RWTH Aachen University, Institute for Theoretical Particle Physics and Cosmology, (TTK), D-52056 Aachen, Germany
[32] INAF Istituto di Radioastronomia, I-40129 Bologna, Italy
[33] Dipartimento di Astronomia, Università di Bologna, I-40127 Bologna, Italy
[34] Università Telematica Pegaso, Piazza Trieste e Trento, 48, I-80132 Napoli, Italy
[35] Centre d'Études Nucléaires de Bordeaux Gradignan, IN2P3/CNRS, Université Bordeaux 1, BP120, F-33175 Gradignan Cedex, France
[36] Department of Physical Sciences, Hiroshima University, Higashi-Hiroshima, Hiroshima 739-8526, Japan
[37] Friedrich-Alexander-Universität Erlangen-Nürnberg, Erlangen Centre for Astroparticle Physics, Erwin-Rommel-Str. 1, D-91058 Erlangen, Germany
[38] Department of Natural Sciences, Open University of Israel, 1 University Road, POB 808, Ra'anana 43537, Israel
[39] Department of Physics and Department of Astronomy, University of Maryland, College Park, MD 20742, USA
[40] Laboratoire de Physique et Chimie de l'Environnement et de l'Espace—Université d'Orléans/CNRS, F-45071 Orléans Cedex 02, France
[41] Station de radioastronomie de Nançay, Observatoire de Paris, CNRS/INSU, F-18330 Nançay, France
[42] The George Washington University, Department of Physics, 725 21st Street NW, Washington, DC 20052, USA
[43] Science Institute, University of Iceland, IS-107 Reykjavik, Iceland
[44] Nordita, Roslagstullsbacken 23, SE-106 91 Stockholm, Sweden
[45] Department of Physics, Graduate School of Science, University of Tokyo, 7-3-1 Hongo, Bunkyo-ku, Tokyo 113-0033, Japan
[46] The Oskar Klein Centre for Cosmoparticle Physics, AlbaNova, SE-106 91 Stockholm, Sweden

[47] Institute of Space Sciences (CSICIEEC), Campus UAB, Carrer de Magrans s/n, E-08193 Barcelona, Spain
[48] Hiroshima Astrophysical Science Center, Hiroshima University, Higashi-Hiroshima, Hiroshima 739-8526, Japan
[49] Max-Planck-Institut für Physik, D-80805 München, Germany
[50] Istituto Nazionale di Fisica Nucleare, Sezione di Roma "Tor Vergata," I-00133 Roma, Italy
[51] Department of Physics and Astronomy, University of Denver, Denver, CO 80208, USA
[52] Osservatorio Astronomico di Trieste, Istituto Nazionale di Astrofisica, I-34143 Trieste, Italy
[53] Department of Physics, University of Johannesburg, P.O. Box 524, Auckland Park 2006, South Africa
[54] Institut für Astro- und Teilchenphysik and Institut für Theoretische Physik, Leopold-Franzens-Universität Innsbruck, A-6020 Innsbruck, Austria
[55] Santa Cruz Institute for Particle Physics, Department of Physics and Department of Astronomy and Astrophysics, University of California at Santa Cruz, Santa Cruz, CA 95064, USA
[56] Department of Physics, The University of Hong Kong, Pokfulam Road, Hong Kong, People's Republic of China
[57] Laboratory for Space Research, The University of Hong Kong, Hong Kong, People's Republic of China
[58] NYCB Real-Time Computing Inc., Lattingtown, NY 11560-1025, USA
[59] Purdue University Northwest, Hammond, IN 46323, USA
[60] Solar-Terrestrial Environment Laboratory, Nagoya University, Nagoya 464-8601, Japan
[61] Institució Catalana de Recerca i Estudis Avançats (ICREA), E-08010 Barcelona, Spain
[62] INAF-Istituto di Astrofisica Spaziale e Fisica Cosmica Bologna, via P. Gobetti 101, I-40129 Bologna, Italy
[63] Dipartimento di Fisica, Università degli Studi di Perugia, I-06123 Perugia, Italy
[64] Praxis Inc., Alexandria, VA 22303, resident at Naval Research Laboratory, Washington, DC 20375, USA
[65] Istituto Nazionale di Fisica Nucleare, Sezione di Trieste, and Università di Trieste, I-34127 Trieste, Italy
[66] Center for Astrophysics and Cosmology, University of Nova Gorica, Nova Gorica, Slovenia
Received 2017 October 25; revised 2018 March 18; accepted 2018 May 13; published 2018 July 6

Abstract

We present the *Fermi* Large Area Telescope (LAT) observations of the binary neutron star merger event GW170817 and the associated short gamma-ray burst (SGRB) GRB 170817A detected by the *Fermi* Gamma-ray Burst Monitor. The LAT was entering the South Atlantic Anomaly at the time of the LIGO/Virgo trigger ($t_{\rm GW}$) and therefore cannot place constraints on the existence of high-energy ($E > 100$ MeV) emission associated with the moment of binary coalescence. We focus instead on constraining high-energy emission on longer timescales. No candidate electromagnetic counterpart was detected by the LAT on timescales of minutes, hours, or days after the LIGO/Virgo detection. The resulting flux upper bound (at 95% C.L.) from the LAT is 4.5×10^{-10} erg cm^{-2} s^{-1} in the 0.1–1 GeV range covering a period from $t_{\rm GW} + 1153$ s to $t_{\rm GW} + 2027$ s. At the distance of GRB 170817A, this flux upper bound corresponds to a luminosity upper bound of 9.7×10^{43} erg s^{-1}, which is five orders of magnitude less luminous than the only other LAT SGRB with known redshift, GRB 090510. We also discuss the prospects for LAT detection of electromagnetic counterparts to future gravitational-wave events from Advanced LIGO/Virgo in the context of GW170817/GRB 170817A.

Key words: gamma-ray burst: general – gamma rays: general – gravitational waves

1. Introduction

Short gamma-ray bursts (SGRBs) have long been thought to be associated with the coalescence of binary compact objects, such as members of neutron star–black hole (NS–BH) and neutron star–neutron star (NS–NS) systems (Paczynski 1986; Eichler et al. 1989; Paczynski 1991; Narayan et al. 1992). This connection arises from considerations of their duration (Norris et al. 1984; Kouveliotou et al. 1993), redshift (Berger 2014a), and host galaxy distributions (Troja et al. 2008; D'Avanzo et al. 2009; Fong & Berger 2013). The observed absence of associated conventional supernovae (Fox et al. 2005; Hjorth et al. 2005a, 2005b; Soderberg et al. 2006; Kocevski et al. 2010; Berger et al. 2013; Troja et al. 2016) has further supported this paradigm. Deep *HST* observations of nearby SGRBs has also provided tantalizing evidence for their association to kilonovae (Metzger et al. 2010; Kouveliotou et al. 2012; Tanvir et al. 2013; Yang et al. 2015; Jin et al. 2016), short-lived infrared transients powered by the radioactive energy of the NS merger ejecta.

The merging of neutron star binaries is predicted to also result in the emission of gravitational waves (e.g., Kobayashi & Mészáros 2003 and references therein), making SGRBs promising candidates for joint gravitational wave (GW) and electromagnetic (EM) detections. For example, the observed orbital decay rate of the binary pulsar PSR B1913+16 is consistent with the predictions of general relativity to better than 10^{-3} precision, setting the date of their merging as ~300 million years from now (Taylor et al. 1979); see Weisberg & Huang (2016) for a recent update.

Strong evidence supporting the long-suspected association of SGRBs and compact binary coalescence was provided on 2017 August 17 when the Advanced Laser Interferometer Gravitational-wave Observatory (LIGO; Abbott et al. 2016b) and Advanced Virgo experiments (Virgo Collaboration 2009) triggered on a compact binary merger candidate (Abbott et al. 2017c) coincident in time with a *Fermi* Gamma-ray Burst Monitor (GBM) detected SGRB, GRB 170817A (Connaughton et al. 2017; Goldstein et al. 2017), which was also detected by *INTEGRAL* SPI-ACS (Savchenko et al. 2017a, 2017b). The joint GW–EM detection has provided the first direct observational evidence connecting SGRBs to neutron star merger events, and has ushered in an exciting era of multi-messenger astronomy. Because gravitational waves probe the system, binding energy and gamma-ray bursts are driven by the configuration of matter

[67] NASA Postdoctoral Program Fellow, USA.
[68] Funded by contract FIRB-2012-RBFR12PM1F from the Italian Ministry of Education, University and Research (MIUR).

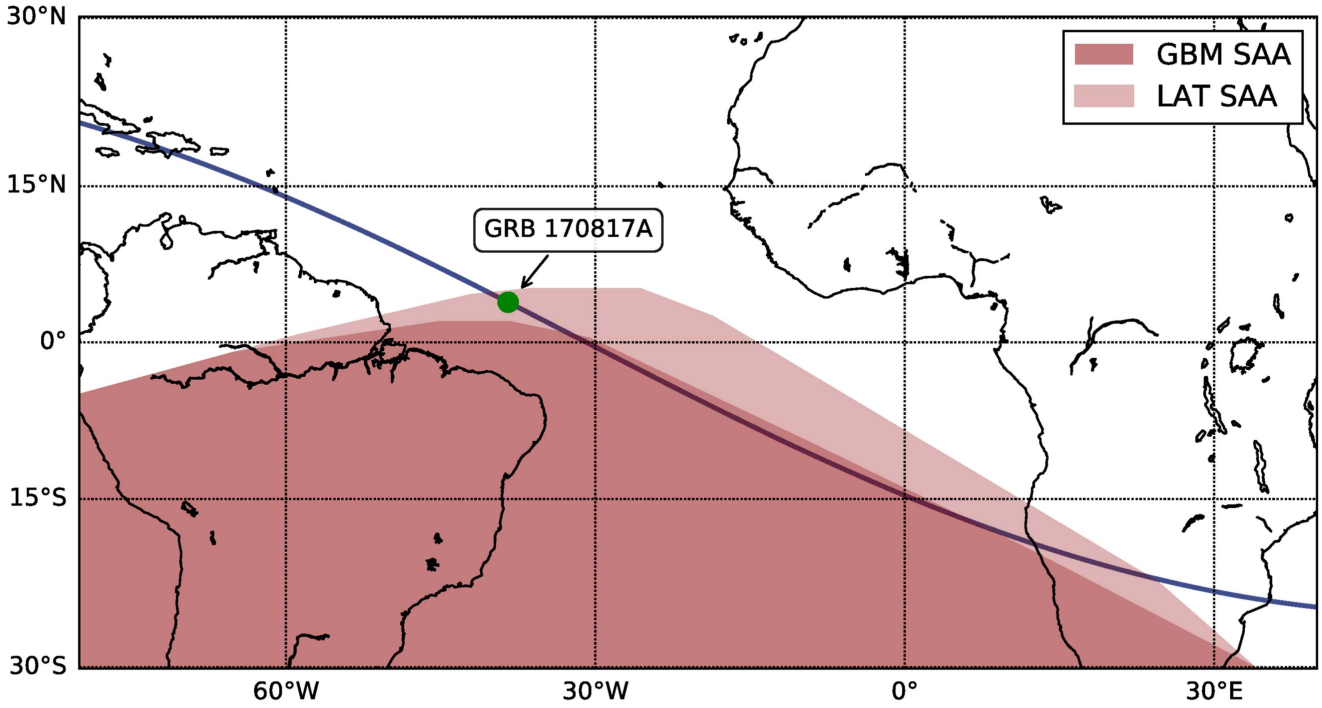

Figure 1. Position of *Fermi* at the trigger time of GRB 170817A (green dot) and its orbital path from west to east. The dark and light red regions define the boundaries of the SAA for the GBM and LAT instruments, respectively. Both instruments do not collect data inside their respective SAA boundaries, due to an elevated charged-particle background.

outside the ultimate event horizon, the combination of such information opens up discovery space concerning tidal disruption of infalling neutron stars, and associated accretion disk and jet formation. It perhaps also offers the prospect for measuring the mass-to-radius ratio and equation of state of a participating neutron star prior to destruction. Shortly after the trigger, the detection of an optical counterpart in the elliptical galaxy NGC 4993 was announced (Abbott et al. 2017a; Coulter et al. 2017a, 2017b) at the position (R.A., decl. = 197.°450354, −23.°381484, J2000). We will assume these coordinates as the location of GW170817 for the remainder of the paper.

The *Fermi* Large Area Telescope (LAT) unfortunately was not collecting data at the time of the LIGO/Virgo and GBM triggers, due to a passage through the South Atlantic Anomaly (SAA), and was thus unable to observe the prompt emission phase of the GRB. The LAT resumed collecting science data $\sim 10^3$ s later, so we focus instead on constraining high-energy emission on longer timescales. We use these limits and the estimated distance of 42.9 ± 3.2 Mpc to NGC 4993 (Abbott et al. 2017b) to set upper limits on the luminosity of the late-time emission of GRB 170817A above 100 MeV.

We describe the details of the data analysis in Section 2, compare GRB 170817A to other LAT-detected SGRBs in Section 3, discuss the prospects of detecting SGRBs associated with future GW triggers in Section 4, and conclude in Section 5.

2. Analysis

2.1. LAT Observations of GW170817

The *Fermi* Gamma-ray Space Telescope consists of two primary science instruments: the GBM (Meegan et al. 2009) and the LAT (Atwood et al. 2009). The GBM comprises 14 scintillation detectors designed to study the gamma-ray sky in the energy band of ∼8 keV–40 MeV. The LAT is a pair conversion telescope consisting of a 4 × 4 array of silicon strip trackers and tungsten converters together with Cesium Iodide (CsI) calorimeters covered by a segmented anticoincidence detector to reject charged-particle background events. The LAT is sensitive in an energy range covering 20 MeV to more than 300 GeV, with a field of view (FOV) of 2.4 sr, observing the entire sky every two orbits (∼3 hr) by rocking north and south about the orbital plane on alternate orbits (Atwood et al. 2009). The LAT detects roughly 15 GRBs per year above 100 MeV, of which ∼1–2 are SGRBs, with localization precisions of ∼10 arcmin (Vianello et al. 2017). The high-energy emission associated with SGRBs is substantially longer in duration with respect to their keV–MeV emission as observed by the GBM, having been detected on timescales of >100 s in two burst sources, and has been proposed to be related to the afterglow phase of the burst (Kumar & Barniol Duran 2009; Ackermann et al. 2013b, 2014; Kouveliotou et al. 2013). The LAT is currently the only instrument that has detected and localized long-lived, high-energy emission from SGRBs, and can substantially reduce the localization uncertainties with respect to GBM, aiding follow-up at other wavelengths.

Fermi-LAT was entering the SAA at the time of the LIGO/Virgo trigger (t_{GW} = 2017 August 17 12:41:04.444 UTC). During SAA passages, the LAT and the GBM do not collect data due to the high-charged-particle background in this region. Because of the higher susceptibility of the LAT to the charged particles in this region, the SAA boundary employed by the LAT encompasses a ∼14% larger area than the boundary used by the GBM, resulting in slightly different times at which the two instruments do not collect data. The GBM and LAT SAA boundaries are illustrated in Figure 1. At the time of the GBM

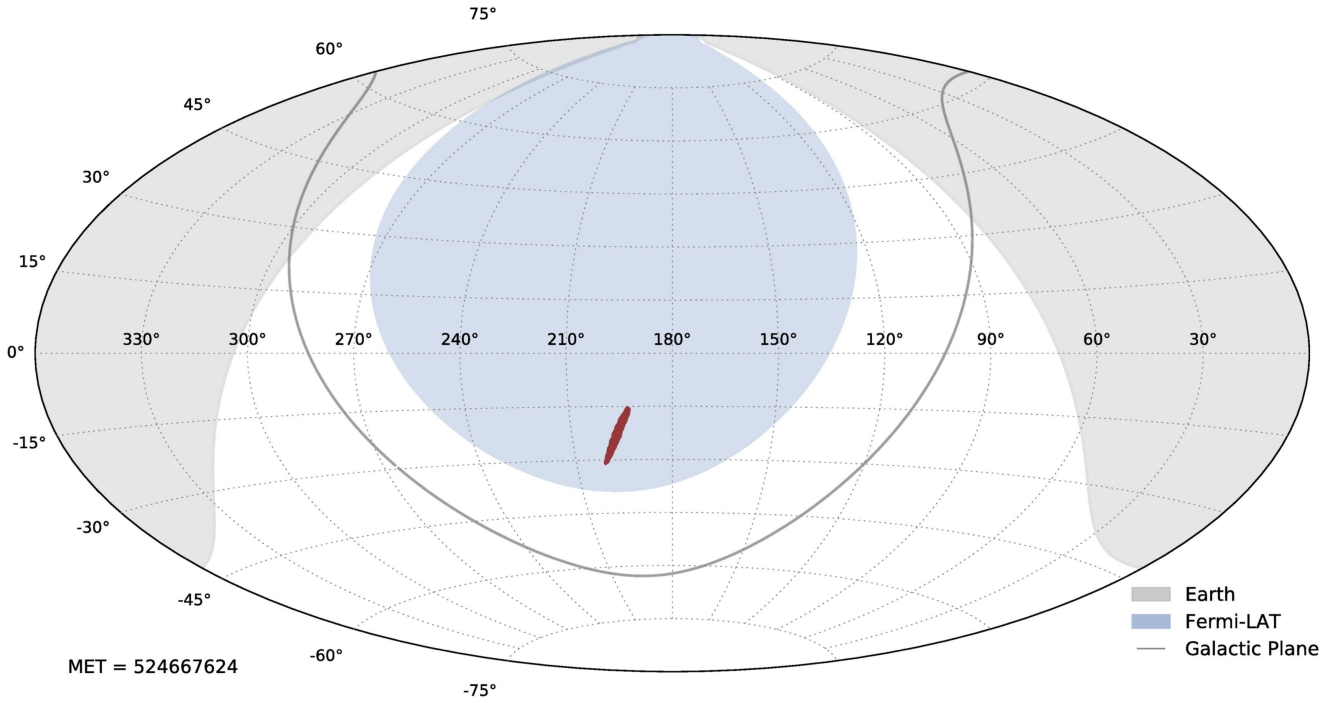

Figure 2. Location of the LAT field of view upon exiting the SAA at $t_{GW} + 1153$ s. The blue and gray regions represent the LAT field of view and the Earth-occulted sky, respectively. The red region represents the final LIGO/Virgo `LALInference` map (90% credible region). The projection is in celestial coordinates and the gray line traces the Galactic plane.

trigger (t_{EM} = 2017 August 17 12:41:06.474598 UTC), the centroid of the final LIGO/Virgo `LALInference` map (Veitch et al. 2015; The LIGO Scientific and Virgo Collaboration et al. 2017) using data from all three gravitational-wave observatories (H1, L1, and V1) was located at R.A. = 197.°25, decl. = −25.°62 (J2000), or Galactic $l = 307.°9$, $b = 37.°1$. This position was $\theta \sim 90°$ from the LAT boresight and outside the nominal $\theta < 65°$ LAT FOV. The LAT resumed data taking upon exiting the SAA at $t_{GW} + 1153$ s. At that time, the entire 90% credible region of the `LALInference` map was within the LAT FOV, and the region subsequently exited at $t_{GW} + 2027$ s. Figure 2 shows the sky coverage of the LAT at $t_{GW} + 1153$ s, when the entire localization region was observed.

2.2. Constraints on the High-energy, Gamma-ray Flux of GRB 170817A

We searched the LAT data for a high-energy, gamma-ray counterpart on different timescales before and after the trigger time, and we computed upper bounds on its flux using an unbinned likelihood analysis described in further detail in Ackermann et al. (2016), Racusin et al. (2017), and Vianello et al. (2017). For all the analyses presented here, we used the `P8_TRANSIENT010E_V6` events class and the corresponding instrument response functions, and the *Fermi* Science Tools version v10r0p5.[69] We furthermore assume a flat ΛCDM cosmology with $H_0 = 67.8$ km s^{-1} Mpc^{-1}, $\Omega_\Lambda = 0.692$ and $\Omega_m = 0.308$ (Planck Collaboration et al. 2016), and a distance to the host of GW170817, NGC 4993, of 42.9 ± 3.2 Mpc (Abbott et al. 2017b), i.e., $z \approx 0.0098$. For the computation of the upper bounds on gamma-ray flux and luminosity, we assume a power-law spectrum with a photon index of −2.

[69] http://fermi.gsfc.nasa.gov/ssc/

We first performed a search for a transient counterpart within the 90% contour of the final LIGO/Virgo `LALInference` map in the time window from $t_{GW} + 1153$ s to $t_{GW} + 2027$ s, the earliest interval in which the region was observed by the LAT, and no significant new sources were found. At the position of the optical counterpart (Abbott et al. 2017a; Coulter et al. 2017a) the value for the flux upper bound over this interval and in the 0.1–1 GeV energy range is 4.5×10^{-10} erg cm^{-2} s^{-1} (95% confidence level), corresponding to an equivalent isotropic luminosity of approximately 9.7×10^{43} erg s^{-1}.

For typical GRBs where the viewing angle is smaller than the jet opening angle, the afterglow is coincident with the end of the prompt emission (Berger 2014a; D'Avanzo 2015), while for jets viewed off-axis, the onset of the afterglows is predicted to be of the order of few days up to 100 days (Granot et al. 2002; van Eerten & MacFadyen 2012). As reported in Troja et al. (2017a; 2017b), an X-ray source positionally coincident with the optical transient was detected at 8.9 days after the GW event, followed by a radio source detection Mooley et al. (2017), suggesting the detection of an afterglow from a possible off-axis jet (Abbott et al. 2017a).

Regardless of the origin of this emission, we monitored the source by performing a likelihood analysis in every interval of time after the trigger when the source was in the LAT FOV. The values of the flux upper bounds vary due to differences in exposures, as shown in Figure 3. In a time period spanning from $t_{EM} - 1$ day to $t_{EM} + 45$ days, these limits range between 9.7×10^{-11} to 3.7×10^{-8} erg cm^{-2} s^{-1}, corresponding to a luminosity range of 2.1×10^{43} to 8.1×10^{45} erg s^{-1} (0.1–1 GeV).

We also examined intervals spanning years before the trigger time. During normal operations, the LAT surveys the entire sky continuously, and has observed the position of GRB 170817A every ∼3 hr since 2008, for a total of ∼55 Ms

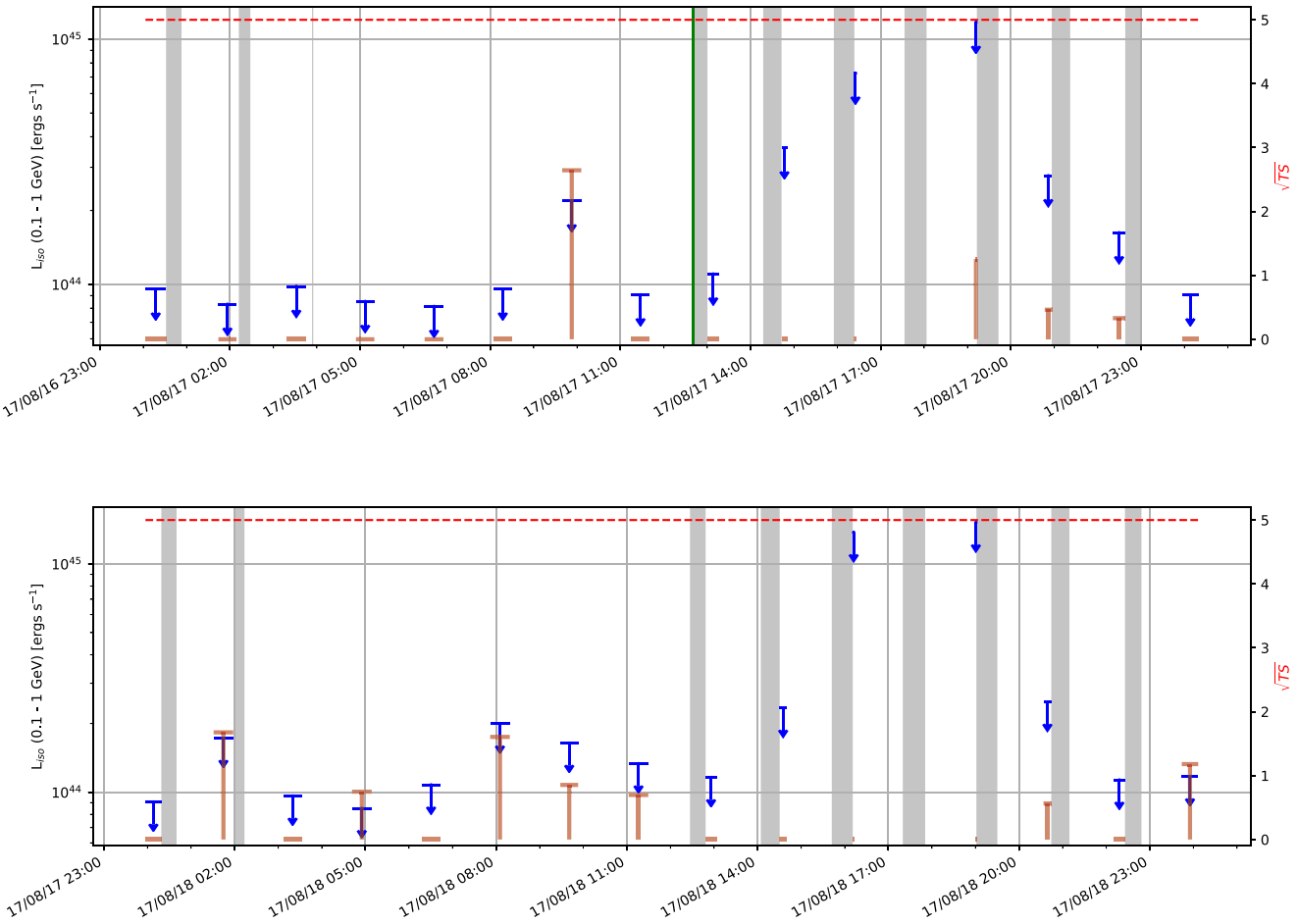

Figure 3. Luminosity in the 0.1–1 GeV energy range upper bounds (blue points, left y-axis) for the first 2 days after t_{EM}. The width of the blue points corresponds to the interval used in the analyses. The red bars of equivalent duration indicate the value of the significance (square root of the Test Statistic TS, right y-axis) in each interval, with the dashed red line representing a value corresponding to approximately 5σ (TS = 25). The gray bands highlight the times when the LAT was in the SAA. The green vertical line in the upper panel is t_{EM}.

of exposure. A search for a counterpart using data collected over the entire lifetime of the mission yielded no detection, returning an upper bound for the average 9 years flux of 1.32×10^{-12} erg cm^{-2} s^{-1} (0.1–1 GeV), corresponding to a luminosity limit of 2.9×10^{41} erg s^{-1}.

We have also looked into the results of the diverse and complementary automatic techniques developed by the *Fermi*-LAT team to continually search for transient events over a variety of timescales. For example, the *Fermi* Autonomous Science Processing (ASP) pipeline performs a search on six hour, one day, and one week timescales to identify candidate gamma-ray sources (Chiang et al. 2007). The candidate sources are subsequently reviewed through a more rigorous likelihood analysis by the Flare Advocate/Gamma-ray Sky Watcher (FA-GSW) pipeline, and positionally cross-checked with known cataloged gamma-ray objects. ASP allows for the detection of flux variations of known cataloged sources, as well as the detection of new unassociated gamma-ray transients. Similar to ASP, the *Fermi* All-sky Variability Analysis (FAVA; Ackermann et al. 2013a) searches for transients over 24 hr and one week timescales.[70] FAVA is a blind photometric technique that looks for deviations from the expected flux in a grid of regions covering the entire sky. The observed long-term, mission-averaged emission serves as reference for the expected flux, allowing the FAVA technique to be independent of any model of the gamma-ray sky. We searched through the full-mission data set for transients detected by ASP and FAVA, positionally consistent with the optical counterpart. No sources with significance greater than 5σ were found. The closest ASP transient is a known gamma-ray source, 3FGL J1312.7−2349, that is associated with the blazar NVSS J131248−235046, roughly 2° from the optical counterpart and therefore unrelated.

3. GRB 170817A in the Context of Other LAT Detected SGRBs

We can compare the properties of GRB 170817A in the context of other GBM and LAT detected bursts. The GBM observations reported in Goldstein et al. (2017) show that the gamma-ray emission from GRB 170817A was softer than that of typical SGRBs, with a peak in its νF_ν spectrum of $E_{peak} = 215 \pm 54$ keV, a value falling in the lowest ∼15th percentile of the SGRB distribution. The burst fluence as measured in the 10–1000 keV energy range is dimmer than typical long bursts, but is consistent with those obtained for other GBM-detected SGRBs.

The GBM has detected over 2000 GRBs in over 9 years of science operations, of which ∼8% have been detected at energies greater than 30 MeV by the LAT. Roughly 17% of the GBM population is made up of SGRBs, with durations

[70] https://fermi.gsfc.nasa.gov/ssc/data/access/lat/FAVA/

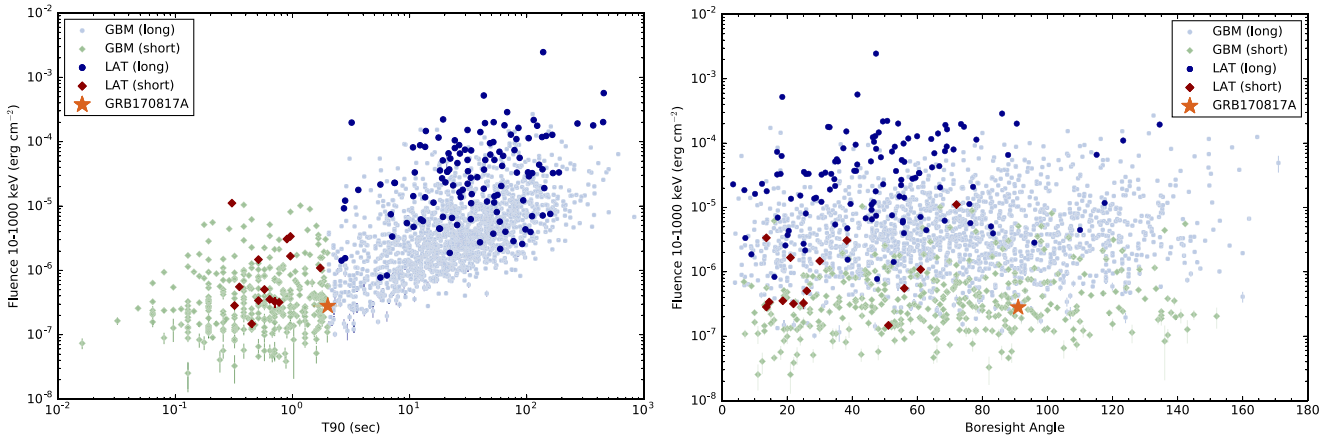

Figure 4. Left panel: the GBM energy fluence (10–1000 keV) plotted against the GBM duration for GRB 170817A (orange star) compared with the LAT-detected short (red diamonds) and long (blue circles) GRBs and non-detected short (light blue circles) and long (light green diamonds) populations of GRBs. Right panel: the GBM energy fluence (10–1000 keV) plotted against angle at which the burst occurred with respect to the LAT boresight at the time of trigger. The LAT detected GRBs with an off-axis angle >65° were outside of the LAT field of view at the trigger time, but were detected after they entered the FOV at a later time.

$T_{90} \leqslant 2$ s in the GBM energy range. The LAT detects ∼5% of the GBM-detected SGRBs. The observed fluence in the 10–1000 keV energy range (Bhat et al. 2016) and duration of the GBM and LAT detected populations can be seen in Figure 4(a). Fluences of SGRBs are generally lower than for long bursts, owing to their shorter durations. The LAT has detected 14 SGRBs with durations shorter than GRB 170817A, eight with comparably low fluence.

Figure 4(a) shows the GBM fluence of the GBM and LAT detected populations plotted versus the angle at which the burst occurred with respect to the LAT boresight at the time of the GBM trigger (T0). Because the LAT sensitivity decreases significantly as a function of increasing boresight angle, the lowest fluence bursts are only detected by the LAT when they occur close to the instrument boresight. The location of the optical counterpart associated with GRB 170817A occurred ∼90° away from the LAT boresight at the time of the GBM trigger. Eight other LAT detected bursts have fluence values as low as GRB 170817A, but a majority of them occurred within $\theta < 25°$ of the LAT boresight, where the instrument is most sensitive. LAT bursts with boresight angles greater than $\theta > 65°$ were either detected using the LAT Low Energy, which provides an additional sensitivity to off-axis photons, or were brought into the FOV through an automatic re-point request of the spacecraft initiated by the GBM for high peak flux.

The LAT detects 1–2 SGRBs per year in the 100 MeV–100 GeV energy range (Ackermann et al. 2013c). Their high-energy emission lasts longer than the prompt emission observed by the GBM, up to ∼200 s after T_0 for the brightest cases. In order to compare GRB 170817A with other LAT detected SGRBs, we compute the flux upper bound in time interval $t_{\rm GW} + 1153$ s to $t_{\rm GW} + 2027$ s in the 100 MeV–100 GeV energy range, obtaining 2×10^{-9} erg cm^{-2} s^{-1} (corresponding to an isotropic luminosity of 4.3×10^{44} erg s^{-1}). The flux upper bound value is above the expected flux at this time from an extrapolation of the power-law temporal decay of the brightest observed SGRB detected by the LAT to date, GRB 090510 (Ackermann et al. 2010; Razzaque 2010). Therefore, the lack of a detection of GRB 170817A at >1000 s is consistent with previous non-detections at this time. We can compare the inferred luminosity upper bound of 4.3×10^{44} erg s^{-1} for GRB 170817A with the luminosity of the extended emission for GRB 090510, also the only LAT-detected SGRB with known redshift ($z = 0.903$). SGRBs in the LAT energy range are typically characterized by a power-law spectrum $\propto E^{-2}$ and a flux decaying as $\propto t^{-1}$ (Ackermann et al. 2013c). By extrapolating the late-time light curve of GRB 090510 (Ackermann et al. 2013c), we estimate the high-energy emission at $T_0 + 1153$ s in its source frame to be roughly 2×10^{48} erg s^{-1}. This effectively rules out late-time emission from GRB 170817A as luminous as GRB 090510.

The lack of such emission is not surprising, though, given that the prompt isotropic equivalent energy observed in the GBM for GRB 170817A of $E_{\rm iso} = 3.0 \pm 0.6 \times 10^{46}$ erg (Goldstein et al. 2017) is six orders of magnitude lower than the value estimated for GRB 090510. GRB 090510 radiated an isotropic equivalent energy of approximately 1.1×10^{53} erg during its prompt emission observed by GBM, and an additional $E_{\rm iso} = 5.5 \times 10^{52}$ erg in the high-energy extended emission detected by the LAT (Ackermann et al. 2013c). This indicates that the reason for the underluminous nature of GRB 170817A must also affect the energetics of the component responsible for the high-energy emission observed by the LAT. Purposed explanations include a relativistic jet viewed off-axis of up to 56° or with an intrinsically low Lorentz factor (Abbott et al. 2017b), a mildly relativistic shock breakout of a cocoon associated with the merger ejecta (Gottlieb et al. 2017; Kasliwal et al. 2017), or the high velocity tail of the neutron rich material dynamically ejected during the merger (Mooley et al. 2018). If we assume a similar ratio between the prompt and extended $E_{\rm iso}$ for GRB 170817A as was determined for GRB 090510 (∼50%), then we would expect a luminosity for the extended emission for GRB 170817A at $t_{\rm GW} + 1153$ s to be on the order of 5×10^{41} erg s^{-1}, well within our estimated luminosity upper bound.

4. Prospects for Future LAT Detections and Sensitivity Study

We now proceed to characterize the sensitivity of the LAT to SGRBs in general. This sensitivity is a function of the characteristics of the LAT, of its background, and of our search methodology. The background level and, consequently, the sensitivity varies across the sky, in particular as a function

of Galactic latitude because of the bright diffuse emission associated with the plane of the Milky Way. We first present the computation of the sensitivity for the optical position of GRB 170817A, which corresponds to a middle Galactic latitude $b = 39.^{\circ}296$. We will then show how the sensitivity changes for typical positions in the sky at lower and higher Galactic latitude. As with all frequentist statistical tests, our method is characterized by the probability of false positives (Type I error, α) and the probability of false negatives (Type-II error, β). We consider an SGRB detected when it has a significance of at least 5σ (TS > 25), i.e., we fix $\alpha = 2.86 \times 10^{-7}$. Following Kashyap et al. (2010), we can then compute the minimum flux that a point source must have in order to be detected above the 5σ level with a given Type-II error probability. We fix for this computation $\beta = 0.5$. We assume an exposure of 100 s, which is roughly the longest duration over which an SGRB has been detected by the LAT in the observer frame. We also assume, for simplicity, that the GRB is close to the axis of the LAT, where the effective area is maximized, and that the pointing is not changing with time. We use as background the Galactic and the Isotropic template provided by the LAT collaboration,[71] representing, respectively, the diffuse emission coming from the Milky Way and the isotropic component generated by particles misclassified as photons and by unresolved sources. We also include all known gamma-ray sources from the 3FGL catalog (Acero et al. 2015) as part of the background. We then simulate repeatedly a point source with a spectrum $dN/dE \propto E^{-2}$, and vary the flux (averaged over the observation) until 50% of the realizations of the simulated source are detected above 5σ. We ascertain that an average flux of $F_s = 9.5 \times 10^{-9}$ erg cm^{-2} s in the 0.1–100 GeV energy range is required to detect a source at mid-latitude with a type II error probability of $\beta = 50\%$ in a 100 s observation. The required flux increases (i.e., the sensitivity decreases) for a source on the Galactic plane by a factor of ∼2–3 (depending on the Galactic longitude), and decreases (i.e., the sensitivity increases) by a factor of ∼2 for a source at the Galactic poles, where the background is lower.

The starting time of a GRB observation is critical because the GRB flux fades rapidly, typically $\propto t^{-1}$. Therefore, we can detect fainter SGRBs the earlier we start observing. In Figure 5, we show how the sensitivity of the LAT for sources at mid-Galactic latitudes changes for five different starting times. The first four shaded regions are for observations with a duration of 100 s, starting, respectively, at T_0, $T_0 + 2$ s, $T_0 + 10$ s, $T_0 + 100$ s, while the last is between $T_0 + 1153$ s and $T_0 + 2027$ s after the trigger time as for GRB 170817A. For reference, we also report the measurements for other SGRBs detected by the LAT, as well as the upper bound for GRB 170817A in the 100 MeV–100 GeV energy range. Among the sample of SGRBs detected by the LAT, we note that the fluences of GRB 081024B and GRB 140402A measured by the GBM in the 10 keV–1 MeV energy band are similar to the one of GRB 170817A. GRB 090510 is the brightest SGRB detected by the LAT so far and resulted in the detection of both its prompt and extended emission. The much dimmer GRB 130804A, on the other hand, was in the field of view at the time of the trigger, but was only detected by the LAT at $T_0 \sim 200$ s, constituting an example of delayed high-energy emission. The statistics are limited, but we can conclude

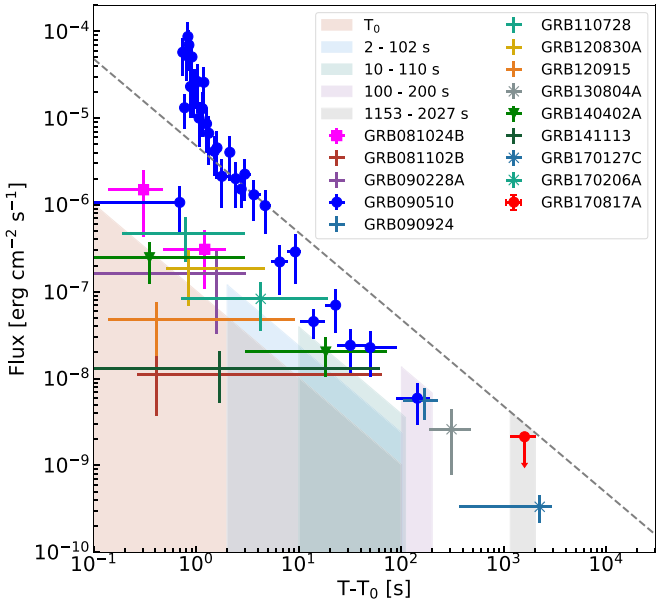

Figure 5. Light curves in the 0.1–100 GeV energy range of the SGRBs detected by the LAT. We highlight GRB 081024B (magenta squares), GRB 140402A (green triangles), GRB 130804 (gray cross), and GRB 090510 (blue circles). The fluence upper bound of GRB 170817A is also shown at the time of the first LAT observation (red circle). The shaded boxes represent the sensitivity to simulated sources detected with TS > 25, 50% of the time. The observation starts at t_0, and 2, 10, 100 s after the trigger and lasts 100 s, as highlighted by the shaded regions. We also computed the sensitivity curve for an observation between 1153 and 2027 s, as for GRB 170817A. This is also extrapolated back in time according to a t^{-1} afterglow decay law (dashed gray line).

that the LAT needs to start observing a source within 100–200 s to have a chance at detecting even the brightest of the LAT-detected SGRBs.

Because the LAT detection efficiency for SGRBs appears to decrease after 100–200 s, we next estimate the probability that the LAT will observe an SGRB within 100 s of the trigger time during normal survey mode. The *Fermi*-GBM observes ∼65% of the sky, with the rest being occulted by the Earth. The LAT observed ∼35% of SGRBs detected by the GBM within ∼100 s of the trigger. Hence, a continuation of this survey strategy indicates that on average, the LAT can observe (either a detection or upper bound) ∼23% of the full-sky SGRB population within 100 s from their GBM trigger. While the population of SGRBs is isotropically distributed, the population of SGRBs within the LIGO/Virgo horizon is likely not. Indeed, the expected horizon for LIGO/Virgo at design sensitivity to BH–NS and NS–NS mergers is estimated to be ∼190 Mpc (Abbott et al. 2017b), and the distribution of galaxies that can potentially host an SGRB is not isotropic within such volume (Bilicki et al. 2014). However, we have performed simulations that showed that such anisotropy does not appreciably affect our observation rate.

The LAT detects ∼5% of all GBM-detected SGRBs. If we assume the LAT will have the same efficiency for GRB/GW triggers and a rate of joint GBM/GW events of 1 (2) per year, we obtain at most a ∼5% (∼10%) probability of detecting one or more GRB/GW with the LAT in one year, respectively. This assumes that GRB/GW events will be representative of the entire GBM-detected SGRB population when observed in gamma-rays.

[71] Available at the *Fermi* Science Support Center (https://fermi.gsfc.nasa.gov/ssc/).

Two important factors pertaining to the detectability of such event by LAT are as follows. (i) *Off-axis viewing*. Since GRB jets propagate at ultra-relativistic speeds with bulk Lorentz factor $\Gamma \gtrsim 100$, the prompt and early afterglow high-energy emission is narrowly beamed with a mean beaming fraction $\langle f_b \rangle = \langle 1 - \cos\theta_0 \rangle \gtrsim 0.015$ corresponding to a mean jet opening angle $\langle \theta_0 \rangle \gtrsim 10^\circ$ (e.g., Berger 2014b). The collimation of SGRBs into narrow jets implies that most GW detections of NS–NS or NS–BH mergers would correspond to jets that do not point toward us, and are instead viewed off-axis, at rather large angles $\theta_{\rm obs}$ from the jet symmetry axis. For such off-axis viewing angles the peak afterglow flux at any given time drops rapidly with increasing $\theta_{\rm obs}$ (Nakar et al. 2002), which makes their detection challenging. The brightness of the off-axis afterglow emission strongly depends on the jet's angular structure, which is not well known for SGRBs (or even for LGRBs for that matter; e.g., Granot 2007). Moreover this brightness should differ between the GBM and LAT wavebands. (ii) *Proximity*. However, given the current sensitivity of the LIGO/Virgo GW detectors, any SGRBs that are observed in coincidence with GW triggers in the future must be relatively nearby with $z < 0.1$ (Abbott et al. 2016a), which improves their detectability (since for a given isotropic equivalent luminosity along our line of sight, $F_\nu \propto D^{-2}$ where D is the source distance). These two effects work in the opposite directions and a careful study is needed to determine the likelihood of such future detections, accounting for D, f_b, and the jet's angular structure.

5. Summary

We present the *Fermi*-LAT observations of the first confirmed LIGO/Virgo binary neutron star merger event GW170817 and the associated SGRB GRB 170817A. Because the LAT was entering the SAA at the time of the LIGO/Virgo trigger, we cannot place constraints on the high-energy ($E > 100$ MeV) emission associated with the moment of binary coalescence. Instead we focus on constraining high-energy emission on longer timescales and report no candidate electromagnetic counterpart above >100 MeV on timescales of minutes, hours, and days after $t_{\rm GW}$. The resulting flux upper bound from the LAT is 4.5×10^{-10} erg cm^{-2} s^{-1} in the 0.1–1 GeV range (and 2×10^{-9} erg cm^{-2} s^{-1} in the 0.1–100 GeV energy range) covering the time interval $t_{\rm GW} + 1153$ s to $t_{\rm GW} + 2027$ s. This limit is above the expected flux at this time from an extrapolation of the power-law temporal decay of the brightest observed SGRB detected by the LAT to date, GRB 090510, which is also the only LAT SGRB with a measured redshift and much more distant ($z = 0.903$). The upper bound on the flux of GRB 170817A corresponds to a luminosity upper bound in the 0.1–1 GeV energy range of 9.7×10^{43} erg s^{-1} (or 4.3×10^{44} erg s^{-1} in the 0.1–100 GeV energy range), significantly lower than the luminosity for GRB 090510 obtained by extrapolating its light curve to 1153 s after the trigger time (4×10^{49} erg s^{-1}). This effectively rules out emission for GRB 170817A as luminous as GRB 090510. However, this is not surprising as the total energy output ($E_{\rm iso}$) during the prompt emission, as measured by the GBM, was 6 orders of magnitude lower for GRB 170817A than for GRB 090510. This might indicate an intrinsically less energetic event or a jet observed off-axis instead of on-axis, or both.

We also looked for a possible high-energy signal in the ∼55 Ms of exposure that the LAT has accumulated at the position of GRB 170817A over the life of the *Fermi* mission. We do not detect any signal from the host galaxy over the entire mission, placing a luminosity upper bound of 2.9×10^{41} erg s^{-1} (0.1–100 GeV). We also did not detect any signal on timescales of minutes, hours or days in the ∼9 years before the trigger time.

The LAT has detected SGRBs with GBM fluences that are comparable to GRB 170817A. Therefore, it is possible for the LAT to detect GRBs characterized by a low-energy prompt emission as faint as GRB 170817A, provided that they have a ratio between low-energy prompt emission and high-energy extended emission similar to previously detected bursts and are observed relatively close to the boresight of the instrument. We have estimated the sensitivity of the LAT to SGRBs and compared it to these previous observations, concluding that the LAT would need to begin observations within ∼100 s from the trigger time.

Finally, under the current observation strategy the LAT should observe ∼23% of the population of SGRBs within 100 s from the trigger, providing meaningful constraints. At the current LAT detection efficiency of ∼5% of all GBM-detected SGRBs (Ackermann et al. 2013c), we estimate that a joint GRB/GW rate of 1 (2) per year would result in at most a ∼5% (∼10%) probability of LAT detecting one or more GRB/GW in one year. This assumes that GRB/GW events are similar to the previously detected population of SGRBs when observed in gamma-rays.

The detection of gravitational waves and an associated EM signal from the coalescence of compact binary system has initiated a new phase in high-energy astrophysics. The discovery of GW170817/GRB 170817A strongly supports the long-suspected association of SGRBs with merging neutron stars. Multi-messenger study of future events can verify this and should impact our understanding of many astrophysical processes—general relativistic dynamics, the equation of state of cold nuclear matter, relativistic jet formation by compact objects, particle acceleration, radioactive heating of the expanding debris (as in kilonovae) and cosmography. We already know that the observations depend strongly upon the orientation of the axes of the binary merger and/or the jet, which can now be determined, at least in principle. Other factors, in particular the initial neutron star masses, spins and magnetization and the environment may also play a role but ought not to be very important. Presuming that there will be an improvement in LIGO-Virgo sensitivity which results in a much larger detection rate and given what we already know from GBM and LAT, there is every reason to believe that gamma-ray observations will drive future developments in this exciting field.

We dedicate this paper to our late friend and colleague, Neil Gehrels, whose curiosity and enthusiasm inspired so much of our work.

The *Fermi* LAT Collaboration acknowledges generous ongoing support from a number of agencies and institutes that have supported both the development and the operation of the LAT as well as scientific data analysis. These include the National Aeronautics and Space Administration and the Department of Energy in the United States, the Commissariat à l'Energie Atomique and the Centre National de la Recherche Scientifique/Institut National de Physique Nucléaire et de

Physique des Particules in France, the Agenzia Spaziale Italiana and the Istituto Nazionale di Fisica Nucleare in Italy, the Ministry of Education, Culture, Sports, Science and Technology (MEXT), High Energy Accelerator Research Organization (KEK) and Japan Aerospace Exploration Agency (JAXA) in Japan, and the K.A. Wallenberg Foundation, the Swedish Research Council and the Swedish National Space Board in Sweden.

Additional support for science analysis during the operations phase is gratefully acknowledged from the Istituto Nazionale di Astrofisica in Italy and the Centre National d'Études Spatiales in France. This work performed in part under DOE Contract DE-AC02-76SF00515.

ORCID iDs

M. Ajello https://orcid.org/0000-0002-6584-1703
L. Baldini https://orcid.org/0000-0002-9785-7726
D. Bastieri https://orcid.org/0000-0002-6954-8862
R. Bellazzini https://orcid.org/0000-0002-2469-7063
E. Bissaldi https://orcid.org/0000-0001-9935-8106
T. J. Brandt https://orcid.org/0000-0003-4087-1786
A. Chekhtman https://orcid.org/0000-0002-6643-9556
C. C. Cheung https://orcid.org/0000-0002-4377-0174
J. Cohen-Tanugi https://orcid.org/0000-0001-9022-4232
F. D'Ammando https://orcid.org/0000-0001-7618-7527
A. Franckowiak https://orcid.org/0000-0002-5605-2219
Y. Fukazawa https://orcid.org/0000-0002-0921-8837
S. Funk https://orcid.org/0000-0002-2012-0080
P. Fusco https://orcid.org/0000-0002-9383-2425
F. Gargano https://orcid.org/0000-0002-5055-6395
D. Gasparrini https://orcid.org/0000-0002-5064-9495
N. Giglietto https://orcid.org/0000-0002-9021-2888
M. Giroletti https://orcid.org/0000-0002-8657-8852
T. Glanzman https://orcid.org/0000-0001-9649-3871
J. Granot https://orcid.org/0000-0001-8530-8941
S. Guiriec https://orcid.org/0000-0001-5780-8770
E. Hays https://orcid.org/0000-0002-8172-593X
M. Kuss https://orcid.org/0000-0003-1212-9998
S. Larsson https://orcid.org/0000-0003-0716-107X
J. Li https://orcid.org/0000-0003-1720-9727
F. Longo https://orcid.org/0000-0003-2501-2270
F. Loparco https://orcid.org/0000-0002-1173-5673
P. Lubrano https://orcid.org/0000-0003-0221-4806
J. D. Magill https://orcid.org/0000-0001-9231-2965
S. Maldera https://orcid.org/0000-0002-0698-4421
A. Manfreda https://orcid.org/0000-0002-0998-4953
M. N. Mazziotta https://orcid.org/0000-0001-9325-4672
T. Mizuno https://orcid.org/0000-0001-7263-0296
M. E. Monzani https://orcid.org/0000-0002-8254-5308
A. Morselli https://orcid.org/0000-0002-7704-9553
I. V. Moskalenko https://orcid.org/0000-0001-6141-458X
N. Omodei https://orcid.org/0000-0002-5448-7577
V. S. Paliya https://orcid.org/0000-0001-7774-5308
M. Pesce-Rollins https://orcid.org/0000-0003-1790-8018
V. Petrosian https://orcid.org/0000-0002-2670-8942
T. A. Porter https://orcid.org/0000-0002-2621-4440
J. L. Racusin https://orcid.org/0000-0002-4744-9898
S. Rainò https://orcid.org/0000-0002-9181-0345
R. Rando https://orcid.org/0000-0001-6992-818X
M. Razzano https://orcid.org/0000-0003-4825-1629
S. Razzaque https://orcid.org/0000-0002-0130-2460
O. Reimer https://orcid.org/0000-0001-6953-1385
F. Ryde https://orcid.org/0000-0002-9769-8016
C. Sgrò https://orcid.org/0000-0001-5676-6214
G. Spandre https://orcid.org/0000-0003-0802-3453
D. J. Suson https://orcid.org/0000-0003-2911-2025
H. Tajima https://orcid.org/0000-0002-1721-7252
D. F. Torres https://orcid.org/0000-0002-1522-9065
G. Tosti https://orcid.org/0000-0002-0839-4126
E. Troja https://orcid.org/0000-0002-1869-7817
J. Valverde https://orcid.org/0000-0002-2345-8888
G. Vianello https://orcid.org/0000-0002-2553-0839

References

Abbott, B. P., Abbott, R., Abbott, T. D., et al. 2016a, ApJL, 832, L21
Abbott, B. P., Abbott, R., Abbott, T. D., et al. 2016b, PhRvL, 116, 131103
Abbott, B. P., Abbott, R., Abbott, T. D., et al. 2017a, ApJL, 848, L12
Abbott, B. P., Abbott, R., Abbott, T. D., et al. 2017b, ApJL, 848, L13
Abbott, B. P., Abbott, R., Abbott, T. D., et al. 2017c, PhRvL, 119, 161101
Acero, F., Ackermann, M., Ajello, M., et al. 2015, ApJS, 218, 23
Ackermann, M., Ajello, M., Albert, A., et al. 2013a, ApJ, 771, 57
Ackermann, M., Ajello, M., Albert, A., et al. 2016, ApJL, 823, L2
Ackermann, M., Ajello, M., Asano, K., et al. 2013b, ApJ, 763, 71
Ackermann, M., Ajello, M., Asano, K., et al. 2013c, ApJS, 209, 11
Ackermann, M., Ajello, M., Asano, K., et al. 2014, Sci, 343, 42
Ackermann, M., Asano, K., Atwood, W. B., et al. 2010, ApJ, 716, 1178
Atwood, W. B., Abdo, A. A., Ackermann, M., et al. 2009, ApJ, 697, 1071
Berger, E. 2014a, ARA&A, 52, 43
Berger, E. 2014b, ARA&A, 52, 43
Berger, E., Fong, W., & Chornock, R. 2013, ApJL, 774, L23
Bhat, P. N., Meegan, C. A., von Kienlin, A., et al. 2016, ApJS, 223, 28
Bilicki, M., Jarrett, T. H., Peacock, J. A., Cluver, M. E., & Steward, L. 2014, ApJS, 210, 9
Chiang, J., Carson, J., & Focke, W. 2007, in AIP Conf. Ser. 921, The First GLAST Symp., ed. S. Ritz, P. Michelson, & C. A. Meegan (Melville, NY: AIP), 544
Connaughton, V., Briggs, M. S., Broida, J., et al. 2017, GCN, 21506, 1
Coulter, D. A., Foley, R. J., Kilpatrick, C. D., et al. 2017b, Sci, 358, 1556
Coulter, D. A., Kilpatrick, C. D., Siebert, M. R., et al. 2017a, GCN, 21529, 1
D'Avanzo, P. 2015, JHEAp, 7, 73
D'Avanzo, P., Malesani, D., Covino, S., et al. 2009, A&A, 498, 711
Eichler, D., Livio, M., Piran, T., & Schramm, D. N. 1989, Natur, 340, 126
Fong, W., & Berger, E. 2013, ApJ, 776, 18
Fox, D. B., Frail, D. A., Price, P. A., et al. 2005, Natur, 437, 845
Goldstein, A., Veres, P., Burns, E., et al. 2017, ApJL, 848, L14
Gottlieb, O., Nakar, E., Piran, T., & Hotokezaka, K. 2017, arXiv:1710.05896
Granot, J. 2007, RMxAC, 27, 140
Granot, J., Panaitescu, A., Kumar, P., & Woosley, S. E. 2002, ApJL, 570, L61
Hjorth, J., Sollerman, J., Gorosabel, J., et al. 2005a, ApJL, 630, L117
Hjorth, J., Watson, D., Fynbo, J. P. U., et al. 2005b, Natur, 437, 859
Jin, Z.-P., Hotokezaka, K., Li, X., et al. 2016, NatCo, 7, 12898
Kashyap, V. L., van Dyk, D. A., Connors, A., et al. 2010, ApJ, 719, 900
Kasliwal, M. M., Nakar, E., Singer, L. P., et al. 2017, Sci, 358, 1559
Kobayashi, S., & Mészáros, P. 2003, ApJ, 589, 861
Kocevski, D., Thöne, C. C., Ramirez-Ruiz, E., et al. 2010, MNRAS, 404, 963
Kouveliotou, C., Granot, J., Racusin, J. L., et al. 2013, ApJL, 779, L1
Kouveliotou, C., Meegan, C. A., Fishman, G. J., et al. 1993, ApJL, 413, L101
Kouveliotou, C., Wijers, R. A. M. J., & Woosley, S. 2012, Gamma-ray Bursts
Kumar, P., & Barniol Duran, R. 2009, MNRAS, 400, L75
Meegan, C., Lichti, G., Bhat, P. N., et al. 2009, ApJ, 702, 791
Metzger, B. D., Martinez-Pinedo, G., Darbha, S., et al. 2010, MNRAS, 406, 2650
Mooley, K. P., Hallinan, G., Corsi, A., et al. 2017, GCN, 21814, 1
Mooley, K. P., Nakar, E., Hotokezaka, K., et al. 2018, Natur, 554, 207
Nakar, E., Piran, T., & Granot, J. 2002, ApJ, 579, 699
Narayan, R., Paczynski, B., & Piran, T. 1992, ApJL, 395, L83
Norris, J. P., Cline, T. L., Desai, U. D., & Teegarden, B. J. 1984, Natur, 308, 434
Paczynski, B. 1986, ApJL, 308, L43
Paczynski, B. 1991, AcA, 41, 257
Planck Collaboration, Ade, P. A. R., Aghanim, N., et al. 2016, A&A, 594, A13
Racusin, J. L., Burns, E., Goldstein, A., et al. 2017, ApJ, 835, 82

Razzaque, S. 2010, ApJL, 724, L109
Savchenko, V., Ferrigno, C., Kuulkers, E., et al. 2017a, ApJL, 848, L15
Savchenko, V., Mereghetti, S., Ferrigno, C., et al. 2017b, GCN, 21507, 1
Soderberg, A. M., Berger, E., Kasliwal, M., et al. 2006, ApJ, 650, 261
Tanvir, N. R., Levan, A. J., Fruchter, A. S., et al. 2013, Natur, 500, 547
Taylor, J. H., Fowler, L. A., & McCulloch, P. M. 1979, Natur, 277, 437
The LIGO Scientific and Virgo Collaboration et al. 2017, GCN, 21527, 1
Troja, E., King, A. R., O'Brien, P. T., Lyons, N., & Cusumano, G. 2008, MNRAS, 385, L10
Troja, E., Piro, L., van Eerten, H., et al. 2017a, Natur, 551, 71
Troja, E., Piro, L., Sakamoto, T., et al. 2017b, GCN, 21787, 1
Troja, E., Sakamoto, T., Cenko, S. B., et al. 2016, ApJ, 827, 102
van Eerten, H. J., & MacFadyen, A. I. 2012, ApJ, 751, 155
Veitch, J., Raymond, V., Farr, B., et al. 2015, PhRvD, 91, 042003
Vianello, G., Omodei, N., Chiang, J., & Digel, S. 2017, ApJL, 841, L16
Virgo Collaboration 2009, Advanced Virgo Baseline Design, Virgo Tech. Rep. VIR-0027A-09, https://tds.ego-gw.it/itf/tds/file.php?callFile=VIR-0027A-09.pdf
Weisberg, J. M., & Huang, Y. 2016, ApJ, 829, 55
Yang, B., Jin, Z.-P., Li, X., et al. 2015, NatCo, 6, 7323